ORGANIC PROCESS RESEARCH & DEVELOPMENT
OPR&D

Full Paper

Drug Loading and Dissolution Properties of Dalcetrapib – Montmorillonite Nanocomposite Microparticles

Katalin Bodnár, Sarah P. Hudson, and Åke C. Rasmuson

Org. Process Res. Dev., **Just Accepted Manuscript** • DOI: 10.1021/acs.oprd.9b00460 • Publication Date (Web): 14 Apr 2020

Just Accepted

is published by the American Chemical Society. 1155 Sixteenth Street N.W., Washington, DC 20036

Drug Loading and Dissolution Properties of Dalcetrapib – Montmorillonite Nanocomposite Microparticles

*Katalin Bodnár, Sarah P. Hudson, Åke C. Rasmuson**

Synthesis and Solid State Pharmaceutical Centre, Department of Chemical Sciences,

Bernal Institute, University of Limerick, Limerick V94 T9PX, Ireland

* *E-mail:* Ake.Rasmuson@ul.ie

ABSTRACT

This work aims to transfer the fast dissolution performances of drug nanosuspensions into the solid state via a carrier particle assisted isolation method and explores the factors affecting the maximum achievable drug loading of the prepared nanocomposite microparticles. The solid composites of fast dissolving dalcetrapib (DCP) nanoparticles on larger montmorillonite (MMT) carrier microparticles have been prepared by an antisolvent precipitation method. The very high dissolution rate of the DCP nanoparticles is combined with the simple solid-liquid separation and drying of the MMT composite microparticles. The fast dissolution rate of DCP from the solid state nanocomposite microparticles was maintained up to a drug loading of 20.9%, and the formulation was stable for a minimum of 10 weeks in the solid state. Surface functionalisation of the MMT particles was not needed for a high and uniform attachment of nanoparticles. Addition of soluble surfactant and polymeric additives, generally used for stabilisation of nanosuspensions, was not required and even decreased the DCP nanoparticle attachment and thus limited drug loading.

Keywords:

Drug nanoparticles, Carrier particles, Antisolvent precipitation, Dissolution rate, Poorly soluble drug, Isolation

1. Introduction

An increasing number of new active pharmaceutical ingredients (APIs) demonstrate poor and inconsistent bioavailability due to their low solubility and dissolution in gastrointestinal fluids, potentially risking API development[1]. The dissolution rates and thus, bioavailability of such APIs can be dramatically improved by increasing the surface-to-volume ratio of the API particles, that is by formulating them as nanoparticles (<1000 nm)[23]. Preparation of nanoparticles using comminution (e.g. wet milling[4], high pressure homogenisation[5]), crystallisation (e.g. liquid antisolvent crystallisation[6,7], supercritical fluid technologies[8]) or combinations of these approaches[9] has been a focus of extensive research. However, isolation of the formed nanoparticles is still an unsolved challenge of the process.

Nanosuspensions are prone to physical instability due to the high surface energy of such systems, resulting in a particle size increase through Ostwald ripening[10] or agglomeration[11,12]. In addition, if the nanosuspension contains a metastable polymorph or amorphous phase, transformation to a more stable phase might occur through a solvent mediated process[13,14]. The presence of API specific soluble additives such as surfactants and polymers generally improves the short term stability of nanosuspensions[15,16,17]. However, in most cases, conversion of the nanosuspension to a solid dosage formulation is required for long term stability and for patient convenience. During this conversion, the small particle size and phase properties must be maintained, as fusion[16] or irreversible agglomeration[18] of nanoparticles during isolation and drying processes would reduce the free surface area and hinder the e improved dissolution

properties. Extensive research has been conducted using freeze drying and spray drying techniques for the isolation of nanoparticles[19,20,21,22]. It has been found that a redispersable product might be obtained with the use of suitable cryoprotectants, lyoprotectants and matrix formers[19,20]. However, despite of the success of these drying processes in academia, the number of industrial applications are limited[23,24]. Freeze drying is a slow and expensive technique[21], while technology and expertise availability may limit the use of spray drying[24]. As an alternative, several isolation strategies have been suggested, including spray granulation with carrier particles[25], fluid bed coating and drying[26,27,28], wet film casting[29], nanoparticle embedment in polymer gels[30], nanoextrusion[31] and carrier particle assisted filtration of nanoparticles[32,33]. Depending on the drug properties, product requirements, technology cost and availability, one can select the most suitable method for isolation.

Carrier particle assisted filtration of nanoparticles provides a simple, inexpensive and industrially feasible process for nanoparticle isolation. Khan et al.[32] introduced the use of insoluble dibasic calcium phosphate as a microparticle carrier for the recovery of ibuprofen and glibenclamide nanoparticles from suspension. In the process, first a drug nanosuspension was prepared either by milling or antisolvent precipitation and stabilised with the use of soluble additives. Then the carrier microparticles were introduced into the nanosuspension to capture nanoparticles on their surfaces and form nanocomposite microparticles that could be easily removed by filtration. Although the improved dissolution properties of the nanoparticles were retained in the dried form, the method was limited by the low drug loading of the composite particles, being only 0.35 w/w%. As a development of this approach, we reported previously a one-step method for carrier particle mediated stabilization and isolation of fenofibrate, mefenamic acid[33] and valsartan[34] nanoparticles using surface functionalised montmorillonite as carrier microparticles in an antisolvent precipitation process. In this process, the use of soluble

additives was not required as the fast attachment of nanoparticles onto the montmorillonite surface stabilised the particles, eliminating the need for a time-consuming additive selection process. However, surface functionalisation of the negatively charged carrier microparticles using a positively charged cationic polymer, protamine sulphate salt, was necessary to improve drug loading of the product nanocomposite microparticles up to 33 w/w% (depending on the specific drug) while maintaining the enhanced dissolution rates due to the high surface area of the nanoparticles.

The above studies introduced the promising concept of carrier mediated nanoparticle isolation, combining simplicity with industrial relevance. However, how the presence of soluble additives and the functionalisation of the carrier particle surface affects the preparation of highly loaded drug–carrier nanocomposite microparticles while maintaining high dissolution rates needs to be explored further. The carrier particles appear to stabilise nanoparticles during the antisolvent precipitation process[33,34] when present during or just after nucleation, without the need for soluble additives. In contrast, some other nanoparticle processes such as wet milling may still require the use of additives if the nanosuspension is not stable during the milling stage, prior to introducing the insoluble carrier[32]. Montmorillonite carrier particles had to be functionalized to preserve the dissolution rates at increased drug loadings for fenofibrate[33] and valsartan[34] but it is unclear whether this is necessary for all drugs or is drug specific.

This work focuses on the filtration based carrier particle supported isolation of nanoparticles, and explores the factors affecting the maximum achievable drug loading of the prepared nanocomposite microparticles while maintaining high dissolution rates. Adding to previous work[32,33,34], the influence of various soluble surfactant and polymeric additives on the crucial step of nanoparticle attachment onto the carrier microparticles is investigated, which highly affects the maximum achievable drug loading of the final product. The work also demonstrates

that the surface zeta potential of drug nanoparticles is critical to obtain a high drug loading onto carrier particles while maintaining high dissolution rates. While previous studies[33,34] have shown the necessity of surface charge modification of the carrier particles for drug nanoparticles with zeta potentials in the range of -25 - -40 mV, this study showed that drug nanoparticles with more moderate zeta potentials (< ~-15 mV) do not require this additional modification. In addition, while in previous work nanoparticle agglomeration was found to be the reason to limit dissolution rates at higher drug loadings of the nanocomposites, this study showed that the dissolution rate can also be limited by partial recrystallization of amorphous particles during the drying process.

At first, the properties of the DCP nanosuspension prepared with optimised antisolvent process parameters are examined in the absence of the carrier montmorillonite (MMT) microparticles. Then, the influence of drug loading and presence of soluble surfactant and polymeric additives on nanoparticle attachment onto the carrier microparticles and on the dissolution behaviour of the fresh suspension are investigated. Finally, the dissolution and solid state properties of the dried nanocomposite microparticles are characterised and the influence of drug loading on the stability during the isolation and drying process is identified.

Dalcetrapib (DCP) is a poorly water soluble (~0.02 µg/mL[35]) cholesterol ester transferase protein inhibitor[36], that was in clinical development for treating cardiovascular diseases by Roche until 2012. Although the original trials did not show a clinical efficacy, it has been found recently that the drug could potentially be beneficial for a genetic subgroup [37]. To our knowledge, a nanoparticle formulation of the drug does not exist.

The carrier microparticle MMT, an insoluble aluminosilicate clay, is widely used in the pharmaceutical industry as a traditional excipient[38] and also extensively studied for use in modified drug delivery systems[39,40,41] due to its low cost, non-toxicity and easy modifiability.

2. Materials and Methods

2.1. Materials

Dalcetrapib (DCP, Form A) was kindly donated by Roche. Ethanol (>99.9) was purchased from Lennox. Methanol (HPLC grade) and sodium chloride (NaCl) was obtained from Fisher. Montmorillonite K10 (MMT, D_{50}=28.0±1.3 μm, determined by laser diffraction method[33]), protamine sulphate salt (PA), polyvinylpirrolidone (PVP, 40kDa) hydroxypropylmethylcellulose (HPMC, 15cP), Pluronic® F127 (PF127), Tween 20, sodium docusate (dioctyl sulfosuccinate sodium salt, DOSS), hydrochloric acid (HCl) and sodium dodecyl sulphate (SDS) was purchased from Sigma Aldrich. Deionised water was used for aqueous solutions (18 MΩ. Elga, purelab Ultra). All chemicals were used as received. The molecular structure of DCP is presented in Figure 1a.

2.2. Preparation of DCP nanoparticles and DCP– MMT nanocomposite microparticles

DCP nanoparticles were prepared by an antisolvent precipitation method and isolated using MMT as carrier microparticles. In a general experiment, DCP solution was prepared by dissolving 60 mg/mL DCP in ethanol. The antisolvent was 9 mL water containing 150 – 1350 mg MMT, equilibrated under agitation for at least 2 h prior to use. DCP nanoparticles were prepared by the quick injection of 1 mL DCP solution at 25.0 ˚C into the antisolvent at 5.0 ˚C under magnetic stirring (1000 rpm). After 1 min aging time, the particles were filtered (Whatman grade 1, 10 μm filter pore), washed with 5 mL water and dried under high vacuum (<27 Pa) at room temperature. Aging time refers to the time elapsed from the injection of drug solution into the antisolvent until sampling the suspension for characterisation or isolation of the particles. A control DCP suspension in the absence of MMT was prepared the same way; however, in this case, isolation of the particles was not possible. Exceptions from this procedure were made when

the antisolvent process parameters were optimised and the influence of soluble additives was studied, detailed below.

At first, the concentration of DCP in the solvent (c_{DCP}) and the antisolvent to solvent ratio (AS/S) was optimised in the absence of MMT and soluble additives by characterising the size of the nanoparticles in suspension at 1 min aging time (Figure S1 in Supplementary information). The experiments were performed at a total final suspension volume of 10 mL, varying c_{DCP} between 30-120 mg/ml and using an AS/S of 9 or 19. From these experiments, the concentration of c_{DCP}=60 mg/mL and AS/S=9 were selected for further studies which conditions offered a good solid load of the suspension (6 mg/ml suspension) at a reasonably small particle size. The short term stability of these particles in suspension was assessed by measuring the particle size at different aging times.

When the influence of additives was studied, the amount of each additive was 2.2 mg/g MMT, unless otherwise specified, at a fixed amount of 225 mg MMT in each experiment. The additives were either present in the antisolvent for more than 2 hours prior to the injection of the drug solution or added to the already prepared suspension as a 1 mL concentrated additive solution in water at 15 s aging time. When the influence of timing of MMT addition on the nanoparticle attachment was investigated, MMT was added as a powder at 15 s aging time to the suspension of nanoparticles, and the suspension was left stirring for an additional 1 min.

The mass of DCP nanoparticles that attached onto MMT particles was indirectly determined by measuring the drug content in the filtrate after filtration. While MMT particles (average size of 28 μm) or DCP nanoparticles that attached onto MMT are retained by a filter with a pore size of 10 μm, DCP nanoparticles that are not attached onto MMT can pass through. Centrifugation was also used to confirm that the carrier particles do not act as a filtration aid but adsorb DCP nanoparticles from suspension. Suspensions of DCP – MMT nanocomposite microparticles were

centrifuged for 1 min at 10000 rpm using a Micro Star 12 Microcentrifuge, conditions that enabled complete settling of MMT particles in the absence of DCP. The filtrate or supernatant was diluted tenfold with methanol to dissolve any DCP particles present and its concentration was determined using a Shimadzu UV-VIS spectrophotometer (λ=246 nm). The percentage of isolated DCP nanoparticles, assumed to attach onto MMT when present, and DCP loading of the composite, that is defined as the actual percentage of DCP nanoparticles in DCP – MMT nanocomposite microparticles, were calculated as the following:

$$m_{DCP}\ \text{isolated (mg)} = m_{DCP}\ \text{total} - m_{DCP}\ \text{filtrate or supernatant} \quad (1)$$

$$\text{isolated DCP (w/w\%)} = (m_{DCP}\ \text{isolated}/m_{DCP}\ \text{total}) \times 100 \quad (2)$$

$$\text{DCP loading (w/w\%)} = (m_{DCP}\ \text{isolated} / (m_{DCP}\ \text{isolated} + m_{MMT})) \times 100 \quad (3)$$

2.3. Characterisation of DCP nanosuspensions in the absence of MMT

The size of DCP particles in suspension in the absence of MMT was characterised by a Malvern Zetasizer Nano ZSP, utilizing a dynamic light scattering technique. At a certain aging time, suspensions were diluted 80 times with water at 5 ˚C, filled into a disposable cuvette, and the temperature was further equilibrated for 120 s at 5 ˚C prior the measurement. Each sample was measured with three consecutive sub-runs at a scattering angle of 173°.

The zeta potential of DCP nanosuspensions in the absence of MMT was determined by a Malvern Zetasizer Nano ZSP, using a folded capillary cell (cell type: DTS1070). The nanosuspension was sampled at 1 min aging time and diluted 20 times using a filtrate of the same formulation (filtered with a 0.2 μm pore sized nylon syringe filter). The temperature was equilibrated for 120 s at 5 ˚C prior to the measurement. Each sample was measured with three consecutive sub-runs. The zeta potential was calculated using the Henry equation with Smoluchowski approximation.

Three separate samples were prepared and analysed for each measurement.

2.4. Characterisation of dried DCP – MMT nanocomposite microparticles, DCP – MMT physical mixtures and as received DCP

The polymorphic form was determined using a Philips PANAlytical X'pert diffractometer. The sample was placed between amorphous tapes and measured in transmission geometry using Ni filtered Cu Kα radiation (λ=1.54 Å), 40 kV accelerating voltage and 40 mA anode current. The diffraction pattern was collected between 5˚ and 30˚ (2θ).

Thermal analysis was performed using a Perkin-Elmer Pyris1 differential scanning calorimeter. Powder containing approximately 1 mg DCP was placed into a closed aluminum pan, and the sample was characterized from 15 °C to 95 °C using 30 mL/min N_2 gas flow and 50 °C/min heating rate. As a control, amorphous DCP was also prepared by cooling the pure melt at a rate of 50 °C/min from 95 °C to 15 °C and characterized at a second reheat of the sample. Calibration was made using indium and the same heating rate. A minimum of five individually prepared samples were characterized to determine the onset temperature and enthalpy of melting. Enthalpy of melting is reported with respect to the amount of DCP in the physical mixture or in the nanocomposite microparticles.

The particle size distribution of as received DCP crystals was determined using a Malvern Morphology G3 in dry mode. A portion of particles was taken out from the bulk after appropriate sample homogenisation. Particles were dispersed on a glass slide using an SUP dispersion unit and 1 bar pressure, and the length and width of 50000 needle-like crystals were measured at a magnification of 2.5 to obtain a representative number based distribution. $D50_{length}$ and $D50_{width}$ are reported as the length and width at which 50% of the crystals are shorter/thinner.

The size and surface architecture of MMT and DCP-MMT composite particles were studied by a HITACHI SU-70 scanning electron microscope (SEM) at 3 kV. To prepare the samples, a small amount of isolated particle was placed onto an adhesive carbon tape attached to a cylindrical aluminum sample holder and gold sputtered at 20 mA for 1 minute using an EMITECH K550.

2.5. Dissolution studies

The solubility of the as received, stable Form A DCP in dissolution media consisting of 0.1 M HCl, 2 g/L NaCl and 2.5 g/L SDS was determined by saturating the solution at 37.0 °C. An excess of solid was added to a stirred solution and equilibrated for 24 h. After 24 hour settling of the solid phase, the supernatant was filtered using a nylon syringe filter (0.2 μm pore size, VWR), discarding the first 3 mL to avoid possible adsorption of the DCP molecules to the filter membrane. The filtrate was diluted with the dissolution media fivefold, and the concentration of DCP was determined using a Shimadzu UV-VIS spectrophotometer (λ=244 nm).

The dissolution of fresh (not isolated) DCP nanosuspensions and different (freshly prepared or isolated to dryness) DCP – MMT formulations was measured by adding an equivalent of 12.5 mg DCP of each sample into 500 mL dissolution media at 37 °C to maintain sink conditions (solubility: 153.2±0.2 μg/mL) and stirring with a magnetic stirrer bar (300 rpm). At specific intervals, a 3 mL aliquot was withdrawn and filtered through a nylon syringe filter (0.2 μm pore

size, VWR) discarding the first 2 mL of the filtrate and analysed by the above mentioned UV-VIS method without dilution. While only the first 15 min of the dissolution experiments are shown in the manuscript for presentation purposes, all samples reached complete dissolution. Suspension samples reached 100±5%, whereas all solid samples reached 100±7% dissolution during the experiments, with the highest error being at low DCP loadings. In the cases of suspensions, the deviation from 100% is likely due to the sampling from unstable suspensions, as the relatively large DCP – MMT nanocomposite microparticles settled quickly when the stirring was stopped. In the cases of solid samples, a lower water content of the processed MMT compared to the unprocessed MMT contributes to the deviation. Thus, for a more accurate comparison of the formulations, all dissolution results were normalized to 100%. Dissolution tests were carried out in triplicate (in the absence of additives), or in duplicate (in the presence of additives).

3. Results

3.1. Nanoparticle formation in the absence of carrier particles

As a first step for the preparation of DCP – MMT nanocomposite microparticles, antisolvent precipitation process conditions were optimised in the absence of MMT in order to achieve a good yield at a reasonably small particle size. From this work AS/S=9 and the DCP concentration of 60 mg/mL selected (Figure S1, supplementary information). The injection of DCP solution into water during the antisolvent precipitation process resulted in the immediate precipitation of the drug, forming a white suspension. Figure 1b presents the particle size distribution of the formed DCP nanoparticles at 1 min aging time, prepared with the optimised process conditions. The average size of these particles was 429±51 nm, while their zeta potential was -14.0±2.5 mV.

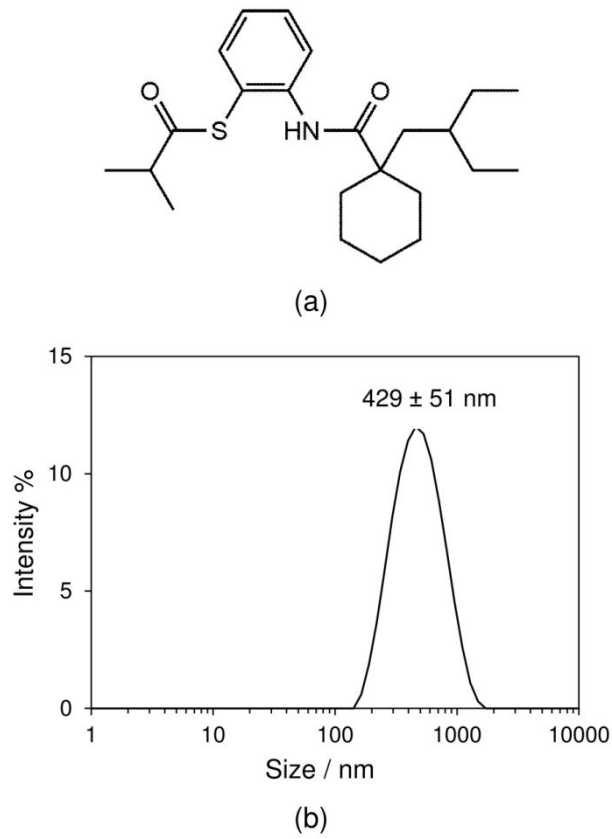

Figure 1 (a) Molecular structure of DCP and (b) particle size distribution of DCP particles at 1 min.

By increasing aging time, the size of the particles first increased from 429 nm to 693 nm within the first 7 min then gradually decreased to 403 nm by 20 min (Figure S2, supplementary information). However, after 3 min, large, visually detectable agglomerates also appeared in the suspension, indicating instability. Since these agglomerates settled quickly after sampling, only the size of small particles coexisting with these large agglomerates (not measurable) were detected by DLS technique at later aging times (>3 min). While stability could be improved in the presence of soluble additives as found in several other API systems[4,17], the duration of stability is not critical for nanoparticle isolation with MMT as shown later.

In the absence of MMT, attempts were made to isolate the nanoparticles at 1 min aging time; however, none of the traditional methods were successful. The nanoparticles blocked the 0.2 μm pore sized filter membrane, and were highly unstable during evaporation drying of a droplet of suspension (at 50 °C or under vacuum (<27 Pa) at room temperature) or freeze drying, forming large crystals. Thus, while formation of the nanoparticles was easy to address using an antisolvent precipitation process due to the high supersaturations generated[42,43], nanoparticle stabilisation in suspension and during isolation was the key challenge to be tackled.

3.2. Nanoparticle attachment onto carrier particles

When present initially in the antisolvent, MMT was highly efficient as a carrier system for capturing DCP nanoparticles. Table 1 reports the actual loading of DCP nanoparticles in the formed DCP – MMT nanocomposite microparticles, depending on the amount of MMT present in the system. The results show that more than 99% of the total amount of DCP (60 mg) was retained even with 150 mg of MMT, corresponding to 28.4% drug loading in the composite. In contrast, in the absence of MMT, 75.6% of DCP passed through the filter paper, resulting in a milky filtrate containing the nanoparticles. The fact that nanoparticles were attaching onto MMT from suspension was also verified by analysing the supernatant of the corresponding suspensions after centrifugation, revealing that 97% of the total amount of DCP did attach to the MMT up to 28.4% composite loading. In contrast, only 56.1% of the particles separated into the bottom sediment under the same conditions in the absence of MMT.

Table 1 Percentage (w/w) of DCP recovered by filtration or by centrifugation at 60 mg DCP and different amount of MMT in the antisolvent – solvent mixture (AS – S), and corresponding DCP loadings in DCP – MMT nanocomposite microparticles (w/w%)

Amount of DCP in AS-S, mg	Amount of MMT in AS-S, mg	DCP isolated by filtration, w/w%	DCP isolated by centrifugation, w/w%	DCP loading in DCP-MMT*, %
60	1350	99.8±0.2	99.8±0.03	4.2
60	450	99.7±0.2	99.0±0.1	11.7
60	225	99.2±0.6	97.7±0.2	20.9
60	190	99.3±0.6	97.6±0.02	23.9
60	150	99.3±0.3	97.2±0.3	28.4
60	100	98.8±0.7	95.4±0.3	37.2
60	Control (no MMT)	24.4±1.6	56.1±3.2	-

* Calculated based on DCP isolation by filtration

Figure 2 shows the influence of soluble surfactant (DOSS, Tween 20) and polymeric (HPMC, PVP, PF127, PA) additives on nanoparticle attachment to MMT. High attachment of DCP nanoparticles onto MMT was maintained in the presence of Tween 20, PVP, PF127 and PA as single additives, shown by the high percentage of isolated particles both by filtration and centrifugation. In contrast, the presence of DOSS as a single additive, and in combination with HPMC and with PVP greatly reduced the attachment to MMT resulting in only 10.1%, 28.1% and 6.7% of the mass of DCP, respectively, separating to the bottom sediment during centrifugation. These values being lower than that of the control suspension (56.1%) indicate that not just particle attachment but also the size of the particles is decreased in the presence of these additives, and these smaller particles would need more time to settle. Interestingly, using filtration instead of centrifugation, a higher amount of DCP was isolated with MMT when DOSS or combination of DOSS with HPMC is used. This was accompanied by a slower filtration time of approximately 3 min and 2 min, respectively, as compared to less than 1 min in the presence of MMT only. In contrast, the combination of DOSS with PVP in the presence of MMT allowed for the nanoparticles to pass through the filter paper, similarly to the control nanosuspension.

When the combination of DOSS with HPMC or PVP was added to the suspension 15 s after the injection of the drug solution into the antisolvent containing MMT, high percentage of the particles could be isolated both with filtration (>98.7%) and centrifugation (>91.5%) showing that the process of nanoparticle attachment to MMT is fast and non-reversible.

When MMT was added at 15 s aging time to the nanosuspension prepared in the absence of additives, the amount of particles that could be isolated both by filtration or centrifugation only reduced by 3% compared to that when MMT was present initially in the antisolvent. In contrast, later addition of MMT to a nanosuspension prepared in the presence of Tween 20, PVP or PF127 resulted in the isolation of only 19.4 – 66.6% DCP by centrifugation, as opposed to the isolation of more than 97.5% DCP when both MMT and the additives were present initially.

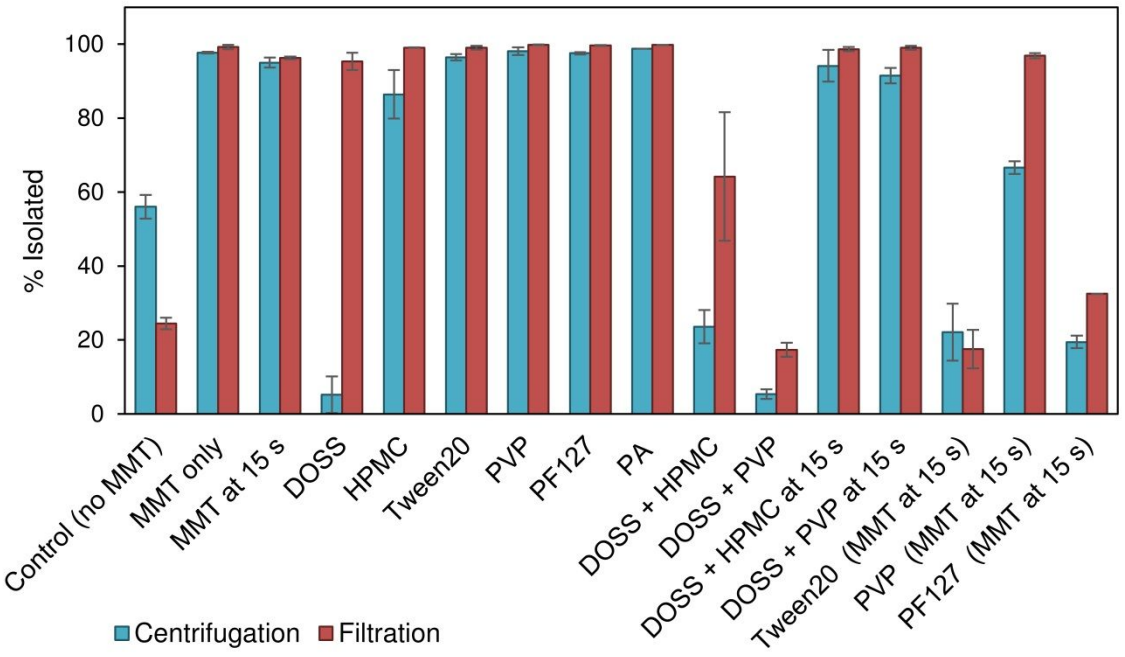

Figure 2 Influence of different additives on the isolation of DCP nanoparticles with MMT particles. Additives added at 2.2 mg/g MMT. Isolation by centrifugation (blue bars) or filtration (red bars). 100% isolation corresponds to a drug loading of 21.1% on MMT. When indicated,

additives were injected as 1 ml concentrated solutions or MMT added as a powder at 15 s aging time.

3.3. Dissolution profiles of drug – carrier nanocomposite microparticles in suspension

In the absence of MMT, the dissolution of the free nanoparticles from a freshly prepared suspension (not isolated) was very fast due to the large surface area of DCP nanoparticles, being complete within 2.2 min (Figure 3). Dissolution of DCP nanoparticles attached onto MMT (from fresh suspension, not isolated) was somewhat slower and the dissolution rate decreased with increasing nanoparticle loading of the composite up to 20.9% DCP. Further increase of the loading to 23.9% and to 28.4% did not have a significant effect on the dissolution profile. Within 15 min, all samples reached 100% dissolution.

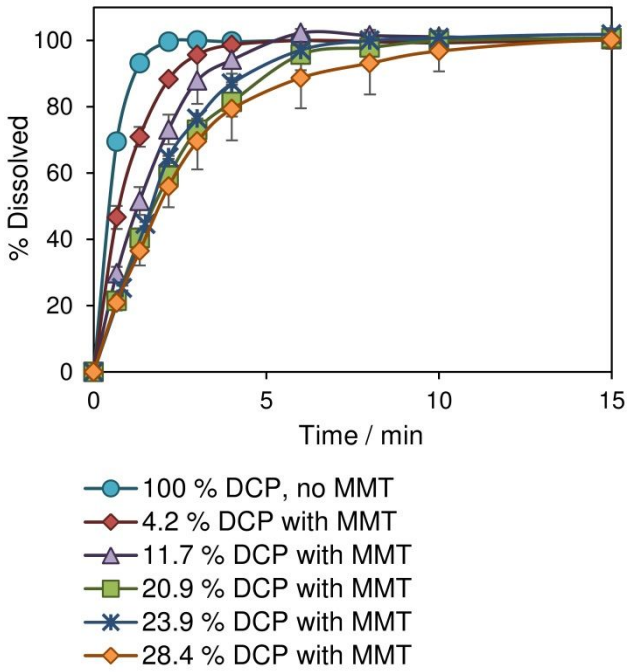

Figure 3 Dissolution behaviour of DCP nanoparticles free in suspension (not isolated) and attached onto MMT in suspension (not isolated) at different DCP loadings of the product nanocomposite microparticles.

The presence of PA or PVP at an amount of 2.2 mg/g MMT, which did not interfere with the high level of nanoparticle attachment, did not show any improvement on the dissolution profile of the freshly prepared suspension at 20.9% drug loading of the nanocomposite microparticles, Figure 4. In addition, in the case of the positively charged surface modifier PA, required for the isolation of negatively charged fenofibrate and mefenamic acid nanoparticles[33], no significant improvement was found even at a decreased DCP nanoparticle loading of 4.2% or increased amount of PA up to 22 mg/g MMT (Figure S3a and S3b in supplementary information, respectively). Dissolution of DCP nanoparticles from a freshly prepared suspension (not isolated) in the presence of MMT was faster with DOSS or with the combination of DOSS and PVP compared to the dissolution profile in the presence of MMT only (Figure 4). However, in these cases, the dissolution rate improvement was associated with the presence of free nanoparticles in suspension, not attached onto MMT, as only a small amount of DCP particles could be isolated by centrifugation in the presence of DOSS or combination of DOSS and PVP (Figure 2, poor isolation efficiency). Thus the dissolution rate improvement with these additives cannot be transferred to an increased dissolution rate in the dried state.

From these results, it is clear that the presence of those soluble additives which maintain high nanoparticle attachment to MMT and thus, high isolation efficiency, cannot improve the dissolution rate of DCP nanoparticles any further.

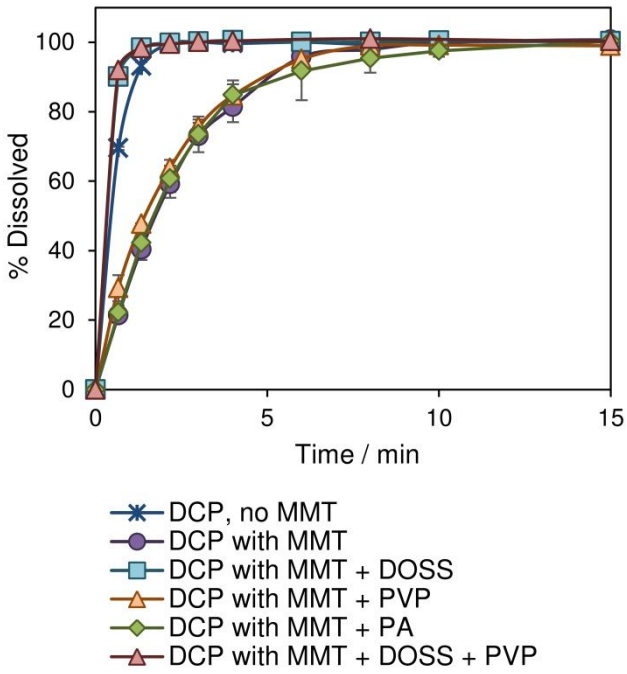

Figure 4 Dissolution profiles of fresh DCP suspension (not isolated) and fresh suspensions of DCP – MMT composites (not isolated) prepared in the presence of selected additives, each at 2.2 mg/g MMT. The ratio of DCP to MMT was equal in all the suspensions, corresponding to a 21.1% DCP loading in DCP – MMT nanocomposites microparticles when 100% is attached. Overlapping dissolution curves: DCP with MMT + DOSS and DCP with MMT + DOSS + PVP; DCP with MMT and DCP with MMT + PVP and DCP with MMT + PA.

3.4. Dissolution profiles of isolated and dried drug – carrier particle composites

DCP – MMT nanocomposite microparticles, free from additional soluble additives, were prepared by an antisolvent precipitation method and isolated using a simple and fast filtration process with an industrially relevant filter pore size (10 μm). Upon addition to the dissolution media, up to DCP loadings of the product composite as high as 20.9%, the dried sample quickly redispersed forming a suspension of composite particles. DCP dissolution from the composites was fast, reproducible and comparable, reaching 80% within the first 5 min and 90% within 15

min (Figure 5). Further increase of the loading to 23.9% resulted in a slightly slower dissolution, reaching 86.8% within 15 min. However, with increasing the loading to 28.4% the dissolution became more variable and slower. The dissolution of the isolated DCP-MMT composite particles is also compared with the dissolution of micron-sized as received DCP crystals, Figure 5. DCP dissolution from the composites was superior to the dissolution of the as received DCP crystals ($D50_{length}$=12.3 µm and $D50_{width}$ =6.23 µm, size data in Figure S4 in supplementary information), the latter only reaching 11.7% in the first 15 min.

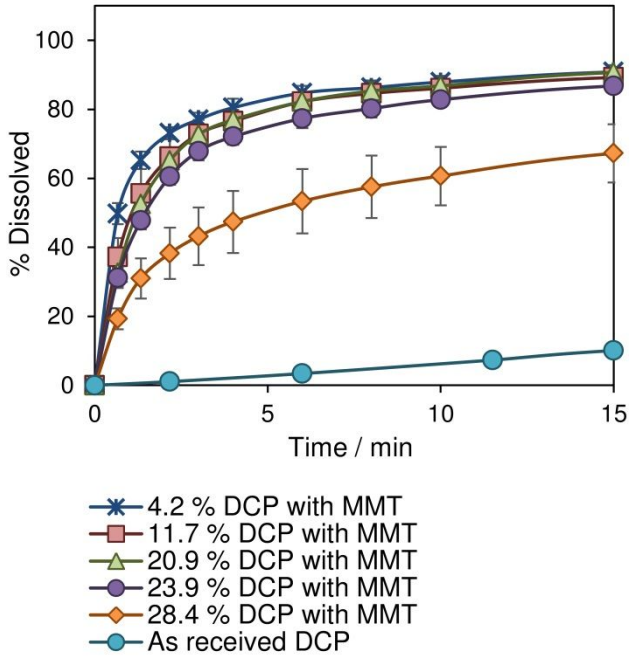

Figure 5 Dissolution of isolated and dried DCP – MMT composites at different DCP loadings and that of the as received DCP crystals.

The improved dissolution of the particles from 20.9% DCP – MMT nanocomposite microparticles remained unchanged after 10 weeks of storage at room conditions, suggesting reasonable stability in the solid state. (Figure S5, Supplementary information).

Comparing the dissolution profiles of DCP – MMT composites in fresh suspensions with those of the dried formulations (Figure S6, supplementary information), at first the dissolution rate is essentially the same at a given drug loading of the composite. However, after the initial period, the dissolution of the dried sample became slower regardless of loading. While the difference in the percentage of dissolved DCP from the fresh suspensions and dried samples was similar and less than 10% at 15 min for 4.2% and 20.9% DCP loadings, it was more than 30% at 28.4% DCP loading, indicating a higher instability of this sample during isolation and drying.

Attempts were made to determine the surface architecture of DCP-MMT composite particles using SEM (Figure 6). Analyses of bare MMT (Figure 6a) revealed that the carrier is composed of larger micron sized particles with a portion of smaller particles attached onto the surface of the large ones (D50=28.0±1.3 μm, determined by laser diffraction method[33]), creating an uneven surface and also implying the presence of voids on the bare MMT structure. On the surface of the composites, Figure 6b, SEM analyses fails to distinguish between DCP and MMT particles.

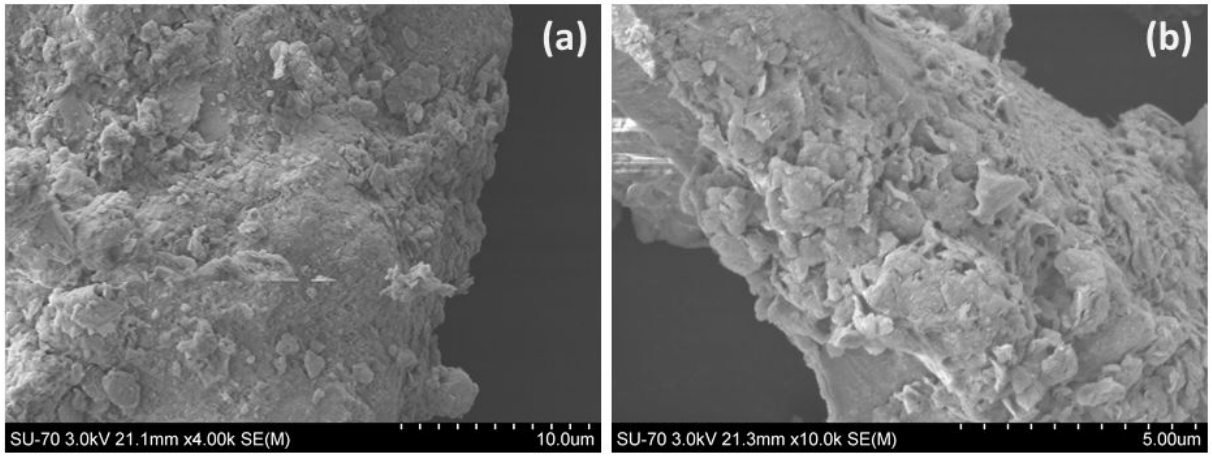

Figure 6. Scanning electron micrographs of bare MMT (a) and DCP – MMT (b) particles

3.5. Crystal structure and crystallinity

To understand the difference in the dissolution profiles of the fresh suspensions and dried formulations, the crystallinity of isolated DCP particles at a composite loading of 20.9%, 23.9% and 28.4% was characterised using PXRD. The PXRD profile of dried DCP – MMT nanocomposite microparticles along with that of the as received DCP and physical mixtures of as received DCP with MMT are presented in Figure 7. As received DCP was in the stable polymorphic form, Form A[44,45], with characteristic peaks at 8.0°, 17.1°, 18.6°, whereas MMT has a strong peak at 26.7°. In the physical mixtures, all the diffraction peaks of DCP were clearly visible with unchanged positions beside the peaks of MMT. The characteristic peaks of Form A DCP were also present in the diffractograms of the composite particles, however, the intensity ratios of DCP and MMT peaks were significantly reduced compared to those of the corresponding physical mixture with the same DCP – MMT ratio, indicating a high amount of amorphous DCP content. In addition, the intensity ratios of the different DCP peaks (*e.g.* the ratio of the Form A peaks at 8.0° and at 18.6°) were also altered revealing altered morphology of the crystalline parts.

In theory, the area (or intensity) ratio of a peak corresponding to DCP and a peak corresponding to MMT should be proportional to the changing weight ratio of DCP to MMT in the composite samples, if the percentage of DCP that is in crystalline state is unchanged. By plotting the area ratio of the DCP peak at 8.0° and that of the MMT peak at 26.7° versus DCP/MMT weight ratios in the composite samples (Figure S7 in supplementary information), a positive deviation from linearity was found suggesting an increasing percentage of crystalline DCP content with increasing DCP loading from 20.9% and 23.9% to 28.4%.

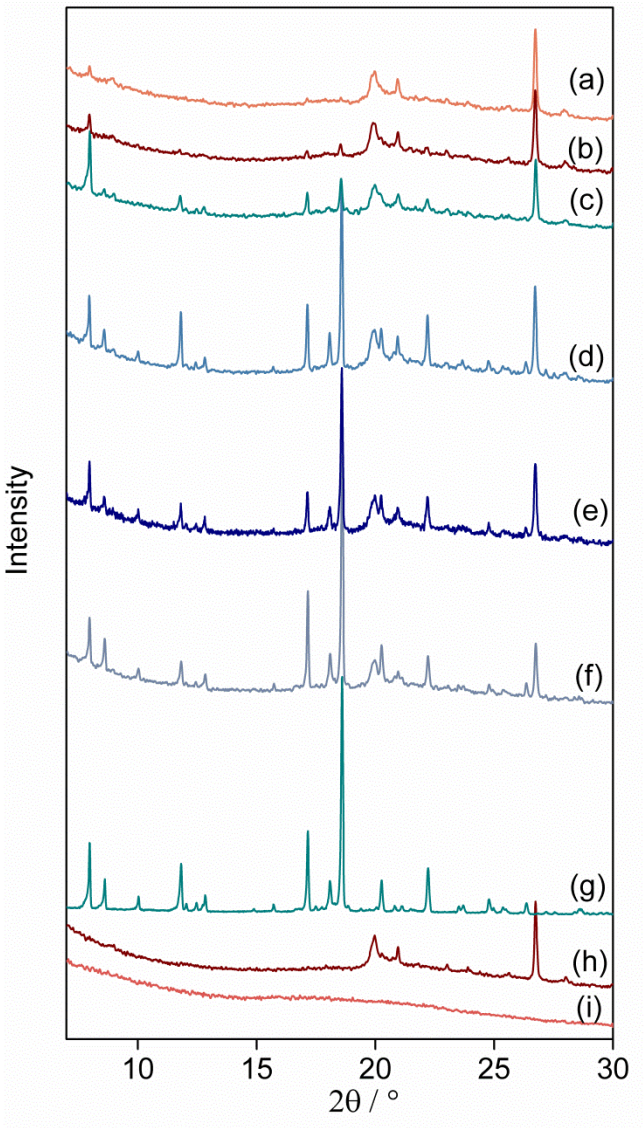

Figure 7 PXRD profiles of DCP – MMT composites: (a) 20.9% DCP with MMT, (b) 23.9% DCP with MMT, (c) 28.4% DCP with MMT; physical mixtures of as received DCP and MMT: (d) 20.9% DCP with MMT, (e) 23.9% DCP with MMT, (f) 28.4% DCP with MMT; (g) pure as received DCP; (h) MMT; (i) background. Intensity of the pure DCP profile has been reduced by a factor of 5 for presentation purposes.

The crystallinity of isolated DCP nanoparticles was also studied by DSC (Figure 8), determining the enthalpy of fusion, ΔH_f, summarised in Table 2. The onset of melting of pure

DCP was 67.9±0.8 °C at a heating rate of 50 °C/min and the enthalpy of melting was ΔH_f=84.6±2.1 J/g (Figure 8, g). Within the temperature range that was selected to monitor the thermal behaviour of DCP, the DSC curve of MMT does not show any thermal events (Figure 8, i), as MMT would have a much higher melting point (>1000 °C). The percentage of crystalline content of DCP attached onto MMT may be calculated by the ratio of enthalpy of fusion of the samples and that of a 100% crystalline reference if no recrystallization of the amorphous phase takes place during heating, and the onset of melting and the enthalpy of fusion of the crystalline DCP is not altered in the presence of MMT[46]. The absence of a melting endotherm of a reheated 100% DCP sample after fast cooling of the melt verifies that the amorphous form does not recrystallize at the applied heating rate (Figure 8, h). The melting onset temperature of DCP physically mixed with MMT (Figure 8, d-f) and DCP – MMT nanocomposite microparticles (Figure 8, a-c) only decreased marginally, by a maximum of 1.5 °C. However, the enthalpy of fusion of the physical mixtures, normalized to the mass of drug present, reduced to 54.1% - 68.1% compared to the pure drug, originating from an interaction between the melted DCP molecules and MMT[47]. The interaction releases heat which partially compensates the energy needed for breaking up molecular interactions in the DCP crystal lattice during melting (endothermic event). This can be seen by the decreased apparent heat of fusion of DCP in the physical mixtures in comparison to the pure DCP. Thus, crystalline content in DCP – MMT nanocomposite microparticles were estimated using the heat of fusion of the corresponding physical mixtures. Important to note, that this method may overestimate crystalline content if, due to spatial arrangement of the crystalline and amorphous DCP particles around MMT, the percentage of molecules interacting with MMT during melting is less than those in the corresponding physical mixtures. With the above mentioned assumption, the crystalline DCP content of the samples at 20.9%, 23.9% and 28.4% drug loadings were estimated to be 9.2±7.2%,

17.9±3.9% and 38.9±11.3%, respectively (Table 2). These values correlate with the amount of undissolved DCP at 15 min, suggesting that the decrease of the dissolution rate above 20.9% DCP loading is governed by an increase of DCP crystallinity.

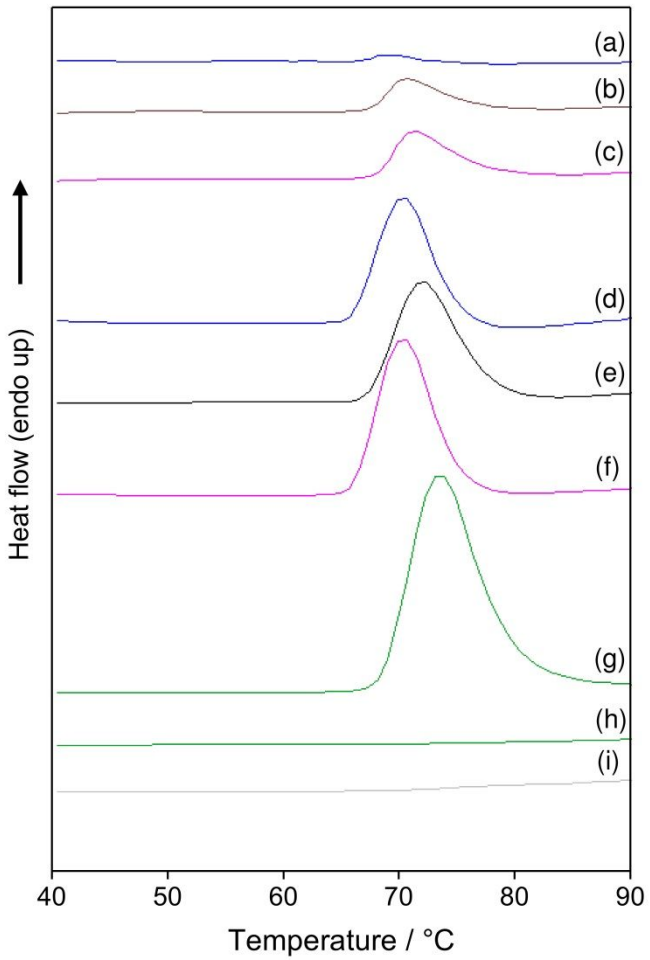

Figure 8 DSC curves showing melting peak of DCP from (a-c) DCP – MMT composites having a DCP content of (a) 20.9%, (b) 23.9%, (c) 28.4%; (d-f) physical mixtures of DCP and MMT at a DCP content of (d) 20.9%, (e) 23.9%, (f) 28.4%; (g) pure DCP; (h) pure DCP at second heating; and (i) DSC curve of MMT.

Table 2 Heat of fusion (ΔH_f) of DCP, on MMT at different loadings ("Sample") and that of physical mixtures of Form A DCP and MMT. ΔH_f of pure Form A DCP is also included. 100% loading refers to the absence of MMT.

DCP loading	ΔH_f, Sample, Jg^{-1}	ΔH_f, Physical mix, Jg^{-1}	Sample crystallinity, %	DCP undissolved after 15 min, %
20.9%	4.0±2.9	43.5±2.6	9.2±7.2	9.3±2.2
23.9%	9.5±1.4	53.2±3.7	17.9±3.9	13.2±1.6
28.4%	22.4±5.1	57.6±3.6	38.9±11.3	32.8±8.5
100%	-	84.6±2.1	-	89.9±0.1

4. Discussion

DCP is a highly hydrophobic drug due to its large hydrocarbon content (Figure 1a). Due to this high hydrophobicity and the only moderate negative zeta potential of the particles in suspension, -14.0±2.5 mV, the nanosuspension is highly unstable. Within a few minutes in the absence of MMT carrier particles or soluble additives, particle growth commences (Figure S2, Supplementary information). By addition of MMT carrier particles, a nanocomposite microparticle is formed, where the fast dissolution rate is maintained, even after isolation and drying. Thus this simple process combines the advantages of nanoparticle stabilization with a filtration based isolation technique.

The aluminosilicate MMT has an expandable layered structure where an octahedral sheet is sandwiched between two tetrahedral sheets[48]. Isomorphous substitution of Si^{4+} with Al^{3+} in the outer siloxane sheet introduces negative charge and hydrophilic patches onto the originally hydrophobic surface[49]. MMT, when present initially in the antisolvent or added 15 s after the injection of drug solution (Table 1 and Figure 2), provides a surface for DCP nanoparticle attachment through hydrophobic interaction between the large hydrocarbon groups of DCP and the hydrophobic siloxane patches[49,50,51]. In addition, interaction of DCP with the MMT surface

through hydrogen bonding is also possible. A favorable interaction between DCP molecules and MMT was also verified by a reduced heat of fusion in the physical mixtures (Table 2). Although the surface of MMT particles bears a significant negative charge (zeta potential: -26.9±1.2 mV[33]), surface functionalisation with the positively charged protamine was not required to achieve high drug loadings at a maintained fast dissolution rate (Figure 4 and Figure S3 in Supplementary information). This can be explained by the less negative charge of DCP nanoparticles compared to that of the previously studied fenofibrate (-25.3±0.9 mV[33]) mefenamic acid (-35.3±1.3 mV[52]) or valsartan (-42.5±1.4 mV[34]) nanoparticles.

While it is hypothesized that DCP nanoparticles adsorb to the MMT surface mainly through hydrophobic interactions, a better understanding of the architecture of the DCP – MMT nanocomposites still needs to be elucidated. Unfortunately SEM analysis, Figure 6, fails to distinguish between API and MMT particles on the surface due to the roughness of the surface of the MMT particles and the immature crystal formation of the API.

Several applications has been described utilizing MMT as an absorber in waste treatment[48], drug delivery and extended release formulations[39,40,41], where ions/molecules are absorbed in the expandable layers of MMT. In our application, however, we rule out the significance of molecular DCP absorption based on the following findings. DCP nanoparticles quickly formed when added to the aqueous phase containing MMT and could be isolated with >99% efficiency within one minute. This isolation efficiency remained the same when MMT was added to the system after precipitation, verifying that interaction occurs with DCP nanoparticles on the outer surface and not with molecular DCP. In addition, dissolution of DCP was fast (90% within 15 min) and complete (reaching 100%) from the composite particles. These data contrasts with extended release formulations where release of adsorbed molecules is observed over several hours[41]. From SEM images of bare MMT (Figure 6a), there are spaces in the uneven surface of

the MMT and between particles on the surface where nanoparticles could become trapped. However, any significant occlusion of the nanoparticles from the bulk dissolution media would slow the subsequent dissolution of the DCP from the nanocomposite, which was not observed.

A selection of soluble additives was studied to cover a wide range of molecular structures and thus interaction abilities that could be categorised as the followings: non-ionic polymer with hydrogen bonding ability (HPMC), non-ionic polymer with no hydrogen bonding ability (PVP), non-ionic block-copolymer (PF127), cationic polymer (PA), non-ionic surfactant (Tween 20), anionic surfactant (DOSS). While the presence of most of the studied additives (Tween 20, PVP, PF127, PA) did not interfere with the high isolation efficiency using MMT, determined both by filtration and centrifugation, attachment to MMT was greatly reduced in the presence of an anionic surfactant DOSS alone or in combination with HPMC or PVP (Figure 2). Adsorption of DOSS ions onto the surface of DCP not only decreases surface hydrophobicity like the adsorption of other uncharged surface active stabilisers[15] but is also expected to increase the negative surface charge of DCP nanoparticles. This in turn increases electrostatic repulsion between DCP nanoparticles and the negative patches of the MMT surface or already attached DCP nanoparticles. Adsorption of DOSS onto the bare MMT surface might also contribute to an increased electrostatic repulsion. Attachment was also reduced when MMT was added 15 s after nanoparticle precipitation in the presence of Tween 20, PVP or PF127, showing that DCP nanoparticles already coated with stabilisers have a lower affinity for interaction with MMT probably due to a lower hydrophobicity of the nanoparticle surface or steric stabilization[12]. These results highlight that the carrier, added to the system prior to or just after the nucleation of the nanoparticles, could attract drug nanoparticles more efficiently when other soluble stabiliser additives are omitted. Thus, the integration of carrier mediated nanoparticle isolation at an early

stage of the formulation development process can eliminate the need for selection of soluble additives for stabilization.

Even directly from the fresh suspension and at low drug loading, DCP loaded nanocomposites have a slightly lower dissolution rate compared to that of the free nanoparticles (Figure 3). The initial dissolution rate over the first 40 seconds has decreased by 30% at 4.2% drug loading (Table 3), and further decreases occur up to 20.9% drug loading. In these experiments the loading is increased by decreasing the amount of MMT, while the amount of DCP remains constant. Accordingly, the reduced dissolution rate is related to the fact that the full surface area of the nanoparticles is not exposed to dissolution, because part of the area is attaching to the MMT surface, and possibly part of the nanoparticles are covered by other DCP particles. This latter becomes more prominent as the DCP loading of the composite increases, further reducing the surface area per unit mass of DCP exposed to dissolution, and thus, the dissolution rate. Above 20,9% loading, however, further decrease in the initial dissolution rate could not be seen, suggesting *e.g.* a looser attachment of DCP nanoparticles in the outer layers and/or an actual release of nanoparticles from the surface during the dissolution.

Table 3 Initial dissolution rates in fresh suspensions at a given drug loading of the DCP – MMT nanocomposite microparticles.

DCP loading, %	Initial dissolution rate, % / min
	104
4.2	70
11.7	45
20.9	32
23.9	30
28.4	31

The relatively moderate decrease of the dissolution rate with increasing loading of the nanocomposite microparticles contrasts with previous work[33], where at higher loadings agglomerated patches of nanoparticles was suggested to be a reason for a more dramatic decrease in dissolution rate.

The isolation and drying of the composite particles do not alter the initial dissolution rate, but certainly increase the time needed for complete dissolution (Figure 3 and Figure 5, compared on Figure S6 in supplementary information). The effect is moderate at low loading but increases at drug loading above 20.9%. This behaviour was found to correlate with increasing crystallinity of the dried DCP particles (Table 2). Accordingly, it is assumed that amorphous nanoparticles form initially in the suspension at all drug loadings, and may completely dissolve from the fresh suspensions (sampled at 1 min) within 15 min. However, after the crystalline form has nucleated the crystals grow at the expense of the amorphous material via a solvent mediated transformation in the suspension or in the wet filter cake[14]. In the system here, this occurs predominantly during the isolation and drying processes (started at 1 min aging time) and leads to a gradually increasing crystalline content. Remaining amorphous material will provide the initial rapid dissolution while the crystalline content having lower solubility and potentially increased size, will have a lower dissolution rate. More crystalline particles are formed at higher loadings in the range of 20.9 – 28.4% drug loading, possibly due to a higher local density of amorphous particles. Besides increasing crystallinity, particle aggregation may also contribute to the decreasing dissolution rates at higher loadings. Once the particles were dried, the crystalline content of the formulation did not change during the studied time period, as shown by their unchanged dissolution profile after 10 weeks storage (Figure S5 in Supplementary information).

When the target particle size distribution of the process is in the nano size with a goal of increasing dissolution rates, stabilisation of the nanoparticles and separation is inherently

challenging. API-MMT nanocomposites reported in this study have been shown to be stable over 10 weeks, can be applied as a technology to a range of APIs and can be produced by simple precipitation and filtration methods. Depending on the applied API[33,34], the composite particles have a maximum API loading above which dissolution rate of the API is compromised, herein being around 20%. Thus, with even further excipients in the final dosage form, the API-MMT nanocomposites proposed here may only be suitable for more potent API molecules. MMT is an FDA approved excipient and has been reported to be good disintegrating agents[53] when used appropriately and a lot more excipients may not be required for tableting. Alternatively a capsule formulation with the API-MMT nanocomposites could also be designed. These further downstream formulation stages are not the focus of the study here but do need to be explored to bring this technology to a higher technology readiness level.

5. Conclusion

Fast dissolving drug (dalcetrapib) – carrier (montmorillonite) nanocomposite microparticles free from soluble additives, were prepared with an antisolvent precipitation method and isolated by a simple, fast, industrially relevant filtration process. In the absence of MMT carrier particles, DCP nanoparticles (429 nm) formed in suspension but were highly unstable and difficult to isolate. MMT carrier particles, when present during or shortly after nanoparticle formation, provided a surface for attachment of the nanoparticles, retaining more than 99% of them up to a corresponding DCP loading of 28.4% in the nanocomposite microparticles. Fast dissolution of isolated DCP nanoparticles, being far superior to that of the larger as received drug crystals, could be maintained even at a drug loading of 20.9% of the composite, with the formulation in dry state being stable for a minimum of 10 weeks of storage. The optimum drug loading was found to be controlled by the interplay of nanoparticle attachment efficiency, drug loading,

dissolution rate of attached nanoparticles and stability during isolation and drying. The use of soluble stabilisers was not required or even decreased nanoparticle attachment, especially when MMT was introduced later to a suspension of stabiliser coated nanoparticles. The MMT surface did not require a surface functionalisation for a uniform nanoparticle attachment and consequently, high dissolution rates, due to a fairly low negative charge of DCP nanoparticles and thus, lack of strong electrostatic repulsion with the negative MMT surface. Thus, this montmorillonite based carrier mediated system can enable solution crystallisation methods for the development of solid dose nanoparticle formulations with high drug content of dalcetrapib, preserving high dissolution rates and having favorable filtration properties.

Acknowledgements

This publication has emanated from research supported in part by a research grant from Science Foundation Ireland (SFI) and is co-funded under the European Regional Development Fund under Grant Number (12/RC/2275).

Declarations of interest: none

Supplementary Information

Supplementary information is available containing optimisation of antisolvent process parameters (Figure S1), size of DCP nanoparticles in suspension over time (Figure S2), influence of different amount of PA on the dissolution of DCP from the composite particles (Figure S3) size of as received DCP crystals (Figure S4), dissolution of DCP from composite particles after 10 weeks storage (Figure S5), comparison of DCP – MMT composite dissolution profiles from

suspensions and dried samples at different DCP loadings (Figure S6), change of PXRD peak ratios of composite samples with increasing DCP loading (S7).

References

1. Kesisoglou, F.; Panmai, S.; Wu, Y. Nanosizing - oral formulation development and biopharmaceutical evaluation. *Adv. Drug Deliv. Rev.* 2007, 59, 631–644.

2. Merisko-Liversidge, E. and Liversidge, G. G. Nanosizing for oral and parenteral drug delivery: a perspective on formulating poorly-water soluble compounds using wet media milling technology. *Adv. Drug Deliv. Rev.* 2011,63, 427–440.

3. Gao, L.; Liu, G.; Ma, J.; Wang, X.; Zhou, L. ; Li, X. Drug nanocrystals: In vivo performances. *J. Control. release* 2012, 160, 418–430.

4. Lestari, M. L. A. D.; Müller, R. H.; Möschwitzer, J. P. Systematic screening of different surface modifiers for the production of physically stable nanosuspensions. *J. Pharm. Sci.* 2015, 104, 1128–1140.

5. Keck, C. M. and Müller, R. H. Drug nanocrystals of poorly soluble drugs produced by high pressure homogenisation. *Eur. J. Pharm. Biopharm.* 2006, 62, 3–16.

6. Thorat, A. A. and Dalvi, S. V. Liquid antisolvent precipitation and stabilization of nanoparticles of poorly water soluble drugs in aqueous suspensions: Recent developments and future perspective. *Chem. Eng. J.* 2012, 181–182, 1–34.

7. D'Addio, S. M. and Prud'homme, R. K. Controlling drug nanoparticle formation by rapid precipitation. *Adv. Drug Deliv. Rev.* 2011, 63, 417–426.

8. Yasuji, T.; Takeuchi, H.; Kawashima, Y. Particle design of poorly water-soluble drug substances using supercritical fluid technologies. *Adv. Drug Deliv. Rev.* 2008, 60, 388–98.

9. Chen, L.; Wang, Y.; Jiaozhen Zhang, J.; Hao, L.; Lou, H.; Zhang, D. Bexarotene nanocrystal-Oral and parenteral formulation development, characterization and

pharmacokinetic evaluation. *Eur. J. Pharm. Biopharm.* 2014, 87, 160–9.

10. Verma, S.; Kumar, S.; Gokhale, R.; Burgess, D. J. Physical stability of nanosuspensions: investigation of the role of stabilizers on Ostwald ripening. *Int. J. Pharm.* 2011, 406, 145–152.

11. Matteucci, M. E.; Hotze, M. A.; Johnston, K. P.; Williams III, R. O. Drug Nanoparticles by Antisolvent Precipitation: Mixing Energy versus Surfactant Stabilization. *Langmuir* 2006, 22, 8951–8959.

12. Wu, L., Zhang, J. and Watanabe, W. Physical and chemical stability of drug nanoparticles. *Adv. Drug Deliv. Rev.* 20011, 63, 456–469.

13. Xia, D.; Wu, J. X.; Cui, F.; Qu, H.; Rades, T.; Rantanen, J.; Yang, M. Solvent-mediated amorphous-to-crystalline transformation of nitrendipine in amorphous particle suspensions containing polymers. *Eur. J. Pharm. Sci.* 2012, 46, 446–454.

14. Lindfors, L.; Skantze, P.; Skantze, U.; Westergren, J.; Olsson, U. Amorphous drug nanosuspensions. 3. Particle dissolution and crystal growth. *Langmuir* 2007, 23, 9866–9874 .

15. Van Eerdenbrugh, B.; Vermant, J.; Martens, J. A.; Froyen, L.; Van Humbeeck, J.; Augustijns, P.; Van den Mooter, G. A screening study of surface stabilization during the production of drug nanocrystals. *J. Pharm. Sci.* 2009, 98, 2091–2103.

16. Tierney, T. B.; Guo, Y.; Beloshapkin, S.; Rasmuson, Å. C.; Hudson, S. P. Investigation of the particle growth of fenofibrate following antisolvent precipitation and freeze–drying. *Cryst. Growth Des.* 2015, 15, 5213–5222.

17. Khan, S.; de Matas, M.; Zhang, J.; Anwar, J. Nanocrystal Preparation: Low-energy

precipitation method revisited. *Cryst. Growth Des.* 2013, 13, 2766–2777.

18. Van Eerdenbrugh, B.; Froyen, L.; van Humbeeck, J.; Martens, J. A.; Augustijns, P.; Van den Mooter, GuyDrying of crystalline drug nanosuspensions-The importance of surface hydrophobicity on dissolution behavior upon redispersion. *Eur. J. Pharm. Sci.* 2008, 35, 127–135.

19. Yue, P.-F. ; Li, G.; Dan, J.-X.; Wu, Z.-F.; Wang, C.-H.; Zhu, W.-F.; Yang, M. Study on formability of solid nanosuspensions during solidification: II novel roles of freezing stress and cryoprotectant property. *Int. J. Pharm.* 2014, 475, 35–48.

20. Kumar, S.; Gokhale, R.; Burgess, D. J. Sugars as bulking agents to prevent nano-crystal aggregation during spray or freeze-drying. *Int. J. Pharm.* 2014, 471, 303–311.

21. Abdelwahed, W.; Degobert, G.; Stainmesse, S.; Fessi, H. Freeze-drying of nanoparticles: formulation, process and storage considerations. *Adv. Drug Deliv. Rev.* 2006, 58, 1688–1713.

22. Cerdeira, A. M.; Mazzotti, M.; Gander, B. Formulation and drying of miconazole and itraconazole nanosuspensions. *Int. J. Pharm.* 2013, 443, 209–220.

23. Chin, W. W. L.; Parmentier, J.; Widzinski, M.; Tan, E. H.; Gokhale, R. A brief literature and patent review of nanosuspensions to a final drug product. *J. Pharm. Sci.* 2014, 103, 2980–2999.

24. Bhakay, A.; Rahman, M.; Dave, R. N.; Bilgili, E. Bioavailability enhancement of poorly water-soluble drugs via nanocomposites : Formulation – processing aspects and challenges. *Pharmaceutics* 2018, 10, 86.

25. Bose, S.; Schenck, D.; Ghosh, I.; Hollywood, A.; Maulit, E.; Ruegger, Colleen Application of spray granulation for conversion of a nanosuspension into a dry powder form. *Eur. J. Pharm. Sci.* 2012, 47, 35–43.

26. Basa, S.; Muniyappan, T.; Karatgi, P.; Prabhu, R.; Pillai, R. Production and in vitro characterization of solid dosage form incorporating drug nanoparticles. *Drug Dev. Ind. Pharm.* 2008, 34, 1209–1218.

27. Azad, M.; Moreno, J.; Bilgili, E.; Davé, R. Fast dissolution of poorly water soluble drugs from fluidized bed coated nanocomposites: Impact of carrier size. *Int. J. Pharm.* 2016, 513, 319–331.

28. Bhakay, A.; Azad, M.; Bilgili, E.; Dave, R. Redispersible fast dissolving nanocomposite microparticles of poorly water-soluble drugs. *Int. J. Pharm.* 2014, 461, 367–379.

29. Sievens-Figueroa, L.; Bhakay, A.; Jerez-Rozo, J. I.; Pandya, N.; Roma, R. J.; Michniak-Kohn, B.; Iqbal, Z.; Bilgili, E.; Davé, R. N. Preparation and characterization of hydroxypropyl methyl cellulose films containing stable BCS Class II drug nanoparticles for pharmaceutical applications. *Int. J. Pharm.* 2012, 423, 496–508.

30. Eral, H. B.; Mahony, M. O.; Shaw, R.; Trout, B. L.; Myerson, A. S.; Doyle, P. S. Composite hydrogels laden with crystalline active pharmaceutical ingredients of controlled size and loading. *Chem. Mater.* 2014, 26, 6213–6220.

31. Khinast, J.; Baumgartner, R.; Roblegg, E. Nano-extrusion : a one-step process for manufacturing of solid nanoparticle formulations directly from the liquid phase. *AAPS PharmSciTech* 2013, 14, 2601-604.

32. Khan, S.; de Matas, M.; Plakkot, S.; Anwar, J. Nanocrystal recovery by use of carrier

particles. *Cryst. Growth Des.* 2014, 14, 1003–1009.

33. Tierney, T.; Bodnár, K.;Rasmuson, Å.; Hudson, S. Carrier particle design for stabilization and isolation of drug nanoparticles. *Int. J. Pharm.* 2017, 518, 111–118.

34. Kumar, A.; Davern, P.; Hodnett, B. K.; Hudson, S. P. Carrier particle mediated stabilization and isolation of valsartan nanoparticles. *Colloids Surfaces B Biointerfaces* 2019, 175, 554–563.

35. Gross, G.; Tardio, J.; Kuhlmann, O. Solubility and stability of dalcetrapib in vehicles and biological media. *Int. J. Pharm.* 2012, 437, 103–9.

36. Shinkai, H.; Maeda, K.; Yamasaki, T.; Okamoto, H.; Uchida, I. Bis(2-(acylamino)phenyl) disulfides, 2-(acylamino)benzenethiols, and S-(2-(acylamino)phenyl) alkanethioates as novel inhibitors of cholesteryl ester transfer protein. *J. Med. Chem.* 2000, 43, 3566–3572.

37. Tardif, J. C.; Rheaúme, E.; Lemieux Perreault, L. P.; Grégoire, J. C.; Feroz Zada, Y.; Asselin, G.; Provost, S.; Barhdadi, A.; Rhainds, D.; L'Allier, P. L.; Ibrahim, R.; Upmanyu, R.; Niesor, E. J.; Benghozi, R.; Suchankova, G.; Laghrissi-Thode, F.; Guertin, M. C.; Olsson, A. G.; Mongrain, I.; Schwartz, G. G.; Dubé, M. P. Pharmacogenomic determinants of the cardiovascular effects of dalcetrapib. *Circ. Cardiovasc. Genet.* 2015, 8, 372–382.

38. R. C. Rowe; P. J. Sheskey; M. E. Quinn, *Handbook of pharmaceutical excipients*, 6th ed. Pharmaceutical Press and American Pharmacists Association, 2009.

39. Jayrajsinh, S.; Shankar, G.; Agrawal, Y. K.; Bakre, L. Montmorillonite nanoclay as a multifaceted drug-delivery carrier: A review. *J. Drug Deliv. Sci. Technol.* 2017, 39, 200–209.

40. Wu, L.; Lv, G.; Liu, M.; Wang, D. Drug release material hosted by natural montmorillonite with proper modification. *Appl. Clay Sci.* 2017, 148, 123–130.

41. Joshi, G. V.; Kevadiya, B. D.; Patel, H. A.; Bajaj, H. C.; Jasra, R. V. Montmorillonite as a drug delivery system: Intercalation and in vitro release of timolol maleate. *Int. J. Pharm.* 2009, 374, 53–57.

42. Dalvi, S. V. and Dave, R. N. Analysis of nucleation kinetics of poorly water-soluble drugs in presence of ultrasound and hydroxypropyl methyl cellulose during antisolvent precipitation. *Int. J. Pharm.* 2010, 387, 172–179.

43. Wang, Z.; Chen, J.-F.; Le, Y.; Shen, Z.-G.; Yun, J. Preparation of Ultrafine Beclomethasone Dipropionate Drug Powder by Antisolvent Precipitation. *Ind. Eng. Chem. Res.* 2007, 46, 4839–4845.

44. Laus, G.; Kahlenberg, V.; Richter, F.; Nerdinger, S.; Schottenberger, H. Improved synthesis and crystal structure of dalcetrapib. *Crystals* 2012, 2, 1455–1459.

45. Neumann, M. A.; van de Streek, J.; Fabbiani, F. P. A.; Hidber, P.;Grassmann, O. Combined crystal structure prediction and high-pressure crystallization in rational pharmaceutical polymorph screening. *Nat. Commun.* 2015, 6, 7793.

46. Baird, J. A. and Taylor, L. S. Evaluation of amorphous solid dispersion properties using thermal analysis techniques. *Adv. Drug Deliv. Rev.* 2012, 64, 396–421.

47. Miriyala, N.; Ouyang, D.; Perrie, Y.; Lowry, D.; Kirby, D. J. Activated carbon as a carrier for amorphous drug delivery: Effect of drug characteristics and carrier wettability. *Eur. J. Pharm. Biopharm.* 2017, 115, 197–205.

48. Zhu, R.; Chen, Q.; Zhou, Q.; Xi, Y.; Zhu, J.; He, H. Adsorbents based on montmorillonite for contaminant removal from water: A review. *Appl. Clay Sci.* 2016, 123, 239–258 .

49. Jaynes, W. F. and Boyd, S. A. Hydrophobicity of siloxane surfaces in smectites as revealed by aromatic hydrocarbon adsorption from water. *Clays Clay Miner.* 1991, 39, 428–436.

50. Sposito, G.; Skipper, N. T.*;* Sutton, R.*;* Park, S.-H.*;* Soper, A. K.*;* Greathouse, J. A. Surface geochemistry of the clay minerals. *Proc. Natl. Acad. Sci.* 1999, 96, 3358–3364.

51. Aguzzi, C.; Cerezo, P.; Viseras, C.; Caramella, C. Use of clays as drug delivery systems: Possibilities and limitations. *Appl. Clay Sci.* 2007, 36, 22–36.

52. Bodnar, K.; Hudson, S. P.; Rasmuson, Å. C. Stepwise use of additives for improved control over formation & stability of mefenamic acid nanocrystals produced by antisolvent precipitation. *Cryst. Growth Des.* 2017, 17, 454–466.

53. Wai, K. N.; Dekay, H. G.; Banker, G. S. Applications of the montmorillonites in tablet making. *J. Pharm. Sci.* 1996, 55, 1244–1248.

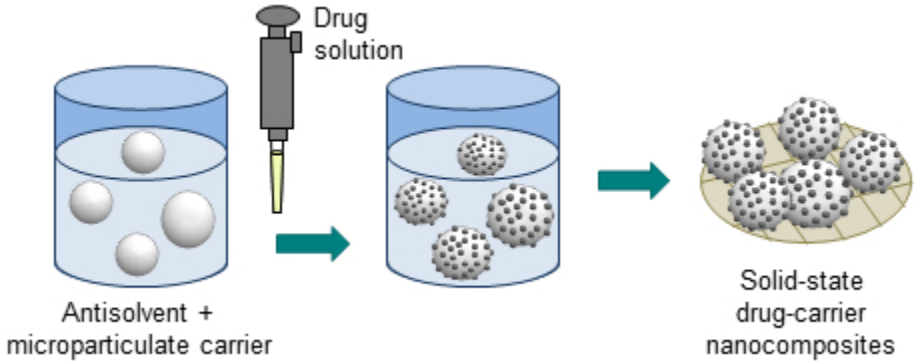

Table of Contents graphic

129x50mm (96 x 96 DPI)